Chinese Physics C

Active spot-scanning test with heavy ions at HIRFL-CSR[*]

DAI Zhong-Ying(戴中颖)[1,2,3]   LI Qiang(李强)[1,3;1)]   LIU Xin-Guo(刘新国)[1,3]

JIN Xiao-Dong(金晓东)[1,3]   HUANG Qi-Yan(黄齐艳)[1,2,3]   XIAO Guo-Qing(肖国青)[1]

[1] Institute of Modern Physics, Chinese Academy of Sciences, Lanzhou 730000, China
[2] Graduate University of Chinese Academy of Sciences, Beijing 100049, China
[3] Key Laboratory of Heavy Ion Radiation Biology and Medicine of Chinese Academy of
Sciences, Lanzhou 730000, China

Abstract: An active spot beam delivery system for heavy ion therapy has been developed based on the Cooling Storage Ring at HIRFL-CSR, where the pencil carbon-ion beams were scanned within a target volume transversely by a pair of orthogonal (horizontal and vertical) dipole magnets to paint the slices of the target volume and longitudinally by active energy variation of the synchrotron slice by slice. The unique techniques such as dose shaping via active energy variation and magnetic deflection constitute a promising three-dimensional conformal even intensity-modulated radiotherapy with heavy ions at HIRFL-CSR. In this paper, the verification of active energy variation and the calibration of steerable beam deflection are shown, as the basic functionality components of the active spot-scanning system. Additionally, based on the capability of creating homogeneous irradiation fields with steerable pencil beams, a radiobiological experiment like cell survival measurement has been performed aiming at comparison of the radiobiological effects under active and passive beam deliveries.

Key words: spot-scanning, heavy ion radiotherapy, beam delivery, active energy variation

PACS: 87.53.Kn, 87.55.ne, 87.56.bd   **DOI:** 10.1088/1674-1137/36/8/018

1 Introduction

Due to the favorite characteristics of heavy ion beams such as inverted depth-dose distribution (Bragg peak) and high relative biological effectiveness, heavy-ion cancer therapy has attracted growing interest all over the world. To make optimal use of these characteristics and to achieve accurate treatment, it is necessary to deliver high doses to tumors selectively while preventing undesired exposure of surrounding normal tissues and organs at risk [1–3]. For this purpose, dynamic spot scanning using pencil beams is indeed an ideal irradiation technique [4–6]. Pencil beam scanning offers better conformation of doses without the need of collimators and compensators and possibly lowers neutron contamination compared with passive beam scattering techniques. Until recently, advanced beam scanning techniques have been available for charged particle radiotherapy. The Gesellschaft fur Schwerionenforschung mbH (GSI) in Germany has commissioned the raster scanning system in the pilot project of carbon ion therapy by deflecting the beam in two dimensions [7]. However, the Paul Scherrer Institute (PSI) in Switzerland has established a spot-scanning system using a deflecting magnet to steer the proton beam in one dimension as the fast scanning and moving the patient couch as the slow scanning in another dimension [8]. Another spot-scanning approach for protons has also been developed at the National Institute of Radiological Sciences (NIRS) in Japan, where proton beams were scanned by the scanning magnets in the lateral

two dimensions in conjunction with changing beam energy with a range shifter [4, 9].

In China, basic research related to heavy-ion cancer therapy and the test experiments of cancer therapy has been carried out at the Institute of Modern Physics (IMP), Chinese Academy of Sciences since 1995. Fruitful achievements have been obtained in the aspects of radiation physics, radiobiology and therapeutic technique [10]. Recently an active spot-scanning beam delivery system has been developed in the deep-seated tumor therapy terminal at HIRFL-CSR. A pencil carbon-ion beam is scanned transversely by horizontal and vertical scanning magnets to deliver the dose to a target volume in combination with active energy variation by the CSR, shifting the Bragg peak of the carbon ions longitudinally. This active dose shaping via active energy variation and lateral beam deflection constitutes a promising three-dimensional conformal and intensity-modulated radiotherapy with heavy ions at HIRFL-CSR. Energy variation of heavy ions actively controls the penatration depths of the Bragg peak and the relationship between the current variation of the scanning magnets and the lateral displacement of beam spots at the iso-center of the therapy terminal is the key point to control the irradiation precisely. In this paper, verification of the active energy variation and calibration of the steerable beam deflection, as the basic functionality of the spot-scanning system, are shown. Additionally, radiobiological experiments such as cell survival measurement were carried out under a uniform irradiation field created by the spot-scanning system in order to compare the radiobiological effect of heavy ions under active and passive beam delivery systems.

2   The materials and methods

2.1   The beam delivery system

At present, HIRFL- CSR achieves its goal of providing carbon ion beams with energies actively changing from 80 to 430 MeV/u with a minimum energy interval of 0.5 MeV/u for therapy. Although the beam at each of the beam energies correspondingly possesses its own beam spot size and the variety of beam size brings flexibility for the treatment planning, the beam size was tuned to be almost the same with a full-width at half maximum (FWHM) of 8–12 mm at the iso-center of the treatment room in the therapy terminal at each energy.

The spot-scanning delivery system developed in the therapy terminal at HIRFL-CSR is shown in

Fig. 1, making up the active beam delivery together with active beam energy variation by CSR. It consists of a pair of orthogonal scanning magnets (SMX and SMY), the main and sub dose monitors, a spot position monitor and an aperture. It should be stated that the magnetic scanning system in the deep-seated tumor therapy terminal can be operated in two patterns such as continuous zigzag [11, 12] and hybrid raster [3] scanning. Therefore, the passive beam shaping using a multi-leaf collimator and range shifter, and the active beam delivery with raster scanning and energy variation by the CSR itself can both be realized. The main and sub dose monitors are nitrogen-filled parallel plate ionization chambers (ICs), 7 μm thick Kapton film coated with aluminum and 1.5 μm thick Mylar film coated with gold as the chamber windows and signal electrodes, respectively. The spot position monitor is a striped IC in which 1.7 mm gold-coated copper strips are used as the signal electrodes, with a spacing of 0.3 mm. The striped IC windows are made of 50 μm Kapton films. In order to achieve an irradiation field large enough at the iso-center, the distances from SMX and SMY to the iso-center were chosen to be 8.38 and 7.66 m, respectively. A beam shutter installed downstream of the scanning magnets is 7.1 m away from the iso-center . The vacuum pipe window, made of 50 μm thick Kapton film, is set 3.1 m upstream of the iso-center. The total water equivalent path length (WEPL) of therapeutic carbon beams passing through the devices from the vacuum pipe window to the iso-center was measured to be approximately 6.8 mm.

In this work, physical performance tests of the active spot-scanning beam delivery system were carried out in two aspects: the energy variation verification in a water phantom using ionization chambers and the beam lateral deflection calibration between nominal excitation currents and scan positions. The experimental setup is schematically shown in Fig. 2.

2.2   The active energy variation and depth-dose distribution measurement

Taking the availability of beam energies and the precise dose management into account, the typical energy interval is chosen to be 7 MeV/u for practical use in the therapeutic energy region. After being injected into CSR in the pattern of "stripped injection", the carbon ions undergo three procedures of accumulation, cooling and acceleration for about 10–12 s for different energies with different parameter settings before the beam experiences the final "slow extraction" procedure. Because the maximum
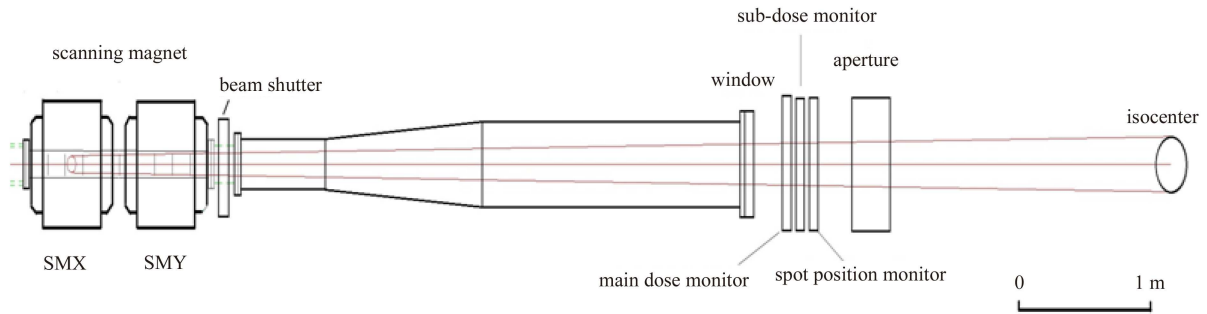
Fig. 1. Layout of scanning beam nozzle of deep-seated tumor therapy terminal at HIRFL-CSR.
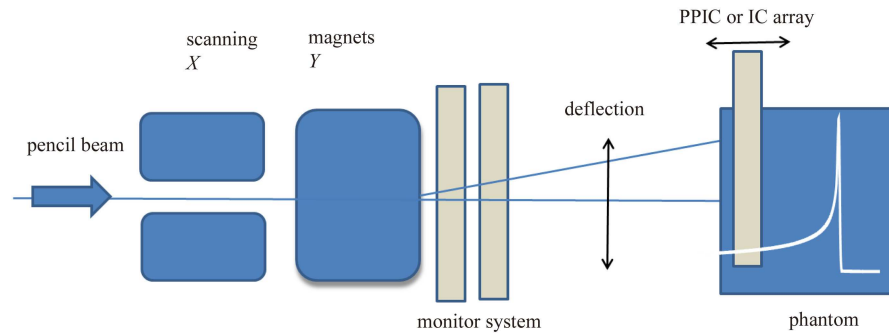
Fig. 2. Schematic diagram of the experimental setup for the spot-scanning test.

duration of the beam extraction is about 5 s, the operation cycle of CSR is about 17 s. In this way, active energy variation is realized by setting different beam-line parameters for CSR.

From the physics point of view, carbon ions with certain energy correspondingly have their specific magnet rigidity as well as the depth-dose distribution in water (tissue), which usually is characterized with a sharp dose rise in the end of their ranges, named the Bragg peak. In other words, energy variation refers to the change of the Bragg peak location in water (tissue) in depth. Therefore, the depth-dose distributions of the carbon ion beams with various energies were measured with double ionization chambers in conjunction with a water tank to be designated to the active energy variation by CSR in this work.

An 8.2 cm diameter parallel-plate ionization chamber system, named Bragg peak chambers (type: thick window 34070 and thin window 34080, PTW-Freiburg, Freiburg, Germany), was used for the measurement of the depth-dose distribution of a carbon ion beam. The Bragg peak chamber 34070 has a nominal sensitive volume of 10.5 cm³ (an effective radius of 40.8 mm and a thickness of 2 mm) and the WEPL of its front window is 4 mm. The chamber 34070 used as the measuring chamber was mounted in one of the drive arms of a 3D water phantom (PTW MP3-P,

Freiburg, Germany) so that the chamber could move along the beam line, while the thin window chamber 34080 used as the reference chamber was mounted on the entrance window outside of the water tank. The water phantom was positioned exactly at the isocenter of the treatment room. The total water equivalent path length(WEPL) before the sensitive volume of the chamber 34070 amounted to 15.9 mm, including the WEPL of the devices located in the beam delivery system, the entrance window of the water tank and the water gap between the interior wall of the tank and the chamber 34070. The measuring accuracy for the depth-dose distributions was 0.1 mm in water due to the minimum accuracy of 0.1 mm for the driving stepper motor of the water tank. The depth dose distributions were measured for the 15 energies 80, 100, 165, 172, 179, 186, 193, 200, 207, 250, 270, 300, 350, 400 and 430 MeV/u for carbon ions using the Bragg peak chambers in combination with the water tank.

2.3 The beam spot and irradiation field measurement

It is the magnetic field induced from the excitation current for the scanning magnet that steers pencil beams with certain magnet rigidities to "paint" a target volume. The corelation between the magnetic

field strength driven by the excitation current and the scan position in the plane perpendicular to the beam line at the iso-center contributes to the beam deflection control which is of extreme importance for the spot-scanning beam delivery system. So the beam spot position control implies strict demands on the scanning magnets and their corresponding power supplies such as stability and flexibility of the current control. The excitation current varies in the range of 0–400 A for both the scanning magnets, and the maximum rise time (−400 A to 400 A) of the current is 9 ms [13]. A maximum field strength of 0.31 T is available for both the scanning magnets at the maximum excitation current. This provides a basis for the estimate of the maximum beam spot deflection at the iso-center. For example, a maximum magnet rigidity of 6.62 T·m can be available for moving the 430 MeV/u carbon ions to the maximum deflection angle of 27 mrad, leading to a maximum displacement of 432 mm at the iso-center.

A planar ionization chamber array of 729 vented plane-parallel detectors (PTW 2D-ARRAY seven29, Freiburg, Germany) was set at the iso-center to measure the lateral deflection position of beam spots. The vented plane-parallel ionization chambers arranged in a matrix of 27×27 are 5 mm×5 mm×5 mm in size, and the center spacing is 10 mm. The IC array covers a field of 280 mm×280 mm, operating with air at atmospheric pressure and room temperature. During measurement, the IC array was mounted in the plane perpendicular to the beam line to detect the pencil beam positions in the lateral direction while the nominal currents supplied for the scanning magnets were controlled through the steering control software.

Using the carbon ion beam of 200 MeV/u, the scanning magnets SMX and SMY were calibrated so as to obtain the relationship between the current and the deflection position of the beam spot at the iso-center, respectively. Then verification of the deflection accuracy was carried out with a matrix of 5×5 scan positions at the iso-center by means of high-resolution radiochromic EBT2 film (International Specialty Products, Wayne, USA), where the center spacing of the adjacent spots was expected to be 20 mm. To demonstrate the maximum irradiation field shaped by the spot-scanning system and check the capability of spot-scanning with arbitrary spacing, a Chinese map and Chinese characters of Lanzhou were delivered to EBT2 films located at the iso-center by the spot-scanning system. Furthermore,

a round-shaped irradiation field of 60 mm in diameter was generated with the 207 MeV/u pencil-like carbon ion beam by the spot-scanning system in order to verify the generation capability of uniform irradiation fields for physical and radiobiological experiments, in which the beam spots were steered to a pre-defined grid of scan points, spaced 3 mm in both vertical and horizontal directions, and the monitor unit (MU) was the same for each scan point.

All the irradiations were performed at room temperature.

2.4 Comparison of cell survival under the spot-scanning and passive beam deliveries

To compare the radiobiological effect induced by carbon ions under the spot-scanning and passive beam deliveries, human salivary gland (HSG) cells were irradiated in the therapy terminal at HIRFL-CSR. The 165 MeV/u carbon ion beam was degraded so as to obtain a dose-average LET of 50 keV/μm for the carbon ions for cell exposure. A uniform irradiation field of 60 mm in diameter was created by the spot-scanning system, where the scan step was set to be 3 mm and the MU at each scan point was determined with a dose optimization algorithm. HSG cells were seeded in 25 cm² culture flasks and irradiated at 0.5, 1.0, 2.0, 3.0 and 4.0 Gy, respectively, after setting the flasks uprightly at the iso-center. Next, a uniform irradiation field was also shaped with continuous zigzag scanning by the scanning magnets operating in the mode of passive beam delivery. HSG cells were also exposed to the carbon ions at the same doses as mentioned above under the passive beam delivery, respectively. Cell survival was determined by means of the standard colony-formation assay.

3 Results

3.1 The depth-dose distributions of carbon ion beams

The depth-dose distributions of the monoenergetic carbon ion beams at the fifteen various energies mentioned above provided by HIRFL-CSR, measured with the combination of the Bragg peak chambers in conjunction with the water tank, are shown in Fig. 3. The corresponding Bragg peak positions of the carbon ions at the 15 energies in depth in water were 17.8, 22.8, 59.2, 63.8, 68.6, 73.5, 78.6, 83.8, 89.0, 123.8, 141.3, 168.9, 218.5, 271.7 and 304.9 mm,
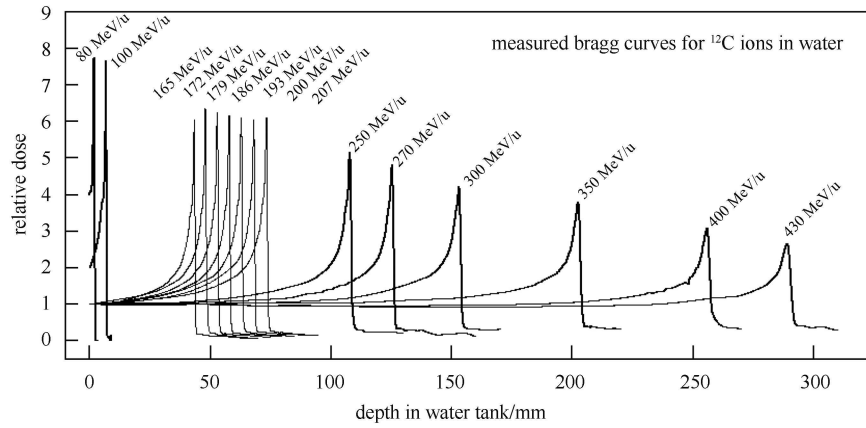
Fig. 3.   Active energy variations with a wide range from 80 to 430 MeV/u by HIRFL-CSR.

respectively, including the 15.9 mm WEPL of the beam delivery system. Clearly, the penetration depth of carbon ion beams of 80–430 MeV/u covers the range from 17.8 to 304.9 mm in water, which is wide enough for tumor therapy. Moreover, the measured depth-dose depths for the carbon ions with the various energies demonstrate that the active energy variation by CSR was realized definitely.

3.2 The beam deflection and field measurements

The relationship between nominal current variation of the scanning magnets and lateral displacement of the beam spots at the iso-center in the therapy terminal was obtained for the carbon ion beams at energies varying from 172 to 207 MeV/u in a spacing of 7 MeV/u. Values of the lateral displacement of the beam spots steered by different excitation currents are displayed in Fig. 4 for the 200 MeV/u carbon ions as an example, where the solid lines are linear fittings to the measured data for the scanning magnets SMX and SMY, respectively. Then the fitted parameters, i.e. the deflection slopes and intercepts, were input into the scanning control system to guide the pencil beams for spot-scanning beam delivery.

To verify the calibrated current-displacement relationship, a 5×5 spot matrix with 20 mm spacing, as shown in Fig. 5(a), was delivered to a radiochromic EBT2 film set at the iso-center by the spot-scanning system for the 200 MeV/u pencil beam. The FWHM of the lateral profile of the single pencil beams at the iso-center was approximately 14 mm. An analysis software named PTW-FilmAnalyze (PTW, Freiburg, Germany) was applied to analyze the accuracy of the spot positions in the EBT2 film. As shown in Fig. 5(b), the five spots in the horizontal direction chosen from the spot matrix were analyzed based on

the grayness gradient. The expected and measured spot positions for the five spots are listed in Table 1. The maximum position deviation for the five spots was found to be 0.8 mm.
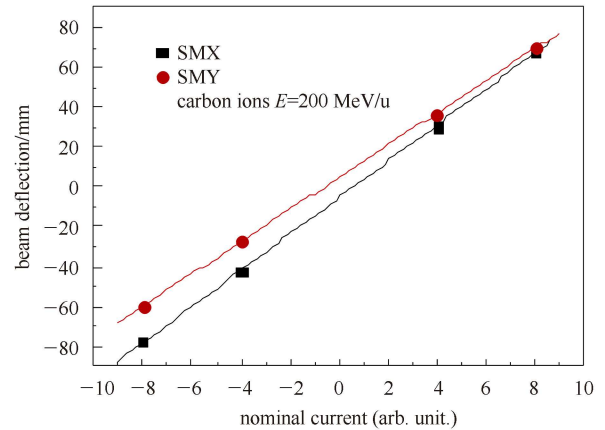
Fig. 4.   The calibration of deflection control for the pair of orthogonal scan magnets using 200 MeV/u carbon ions.

Table 1.   Spot-scanning deflection verification.

No	spot position		deviation/mm
	expected/mm	measured/mm	
1	−40.0	−39.2	0.8
2	−20.0	−19.6	0.4
3	0.0	0.0	0.0
4	20.0	19.6	0.4
5	40.0	40.4	0.4

Shown in Fig. 6 are the arbitrary contours such as a Chinese map and the Chinese characters of Lanzhou shaped successfully by the spot-scanning beam delivery technique. These arbitrary contours confirm that not only the maximum irradiation field could reach up to 20 cm×20 cm by the spot scanning system, but also its performance could meet the basic requirement for spot-scanning beam delivery.
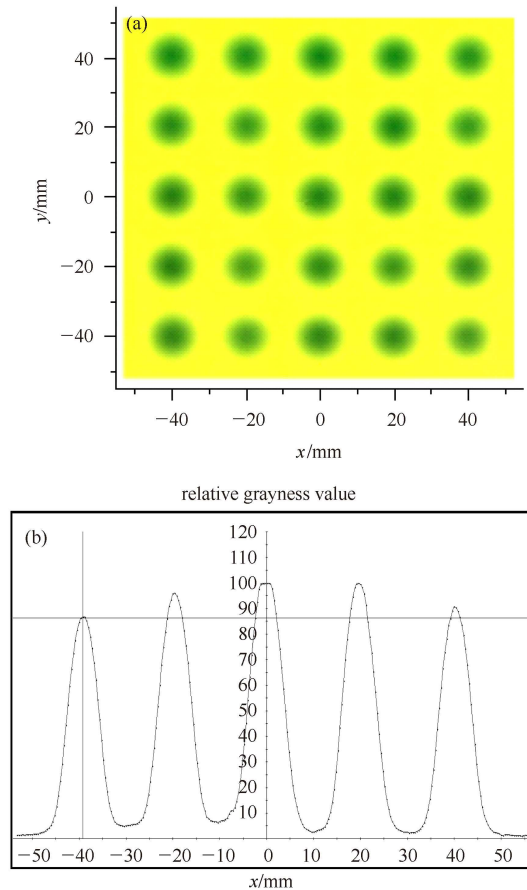
Fig. 5. Example of spot position measurements. (a) The 5×5 dots matrix of 20 mm spot spacing measured by using radiochromic film. (b) The example of the analysis procedure of spot-scanning position accuracy.
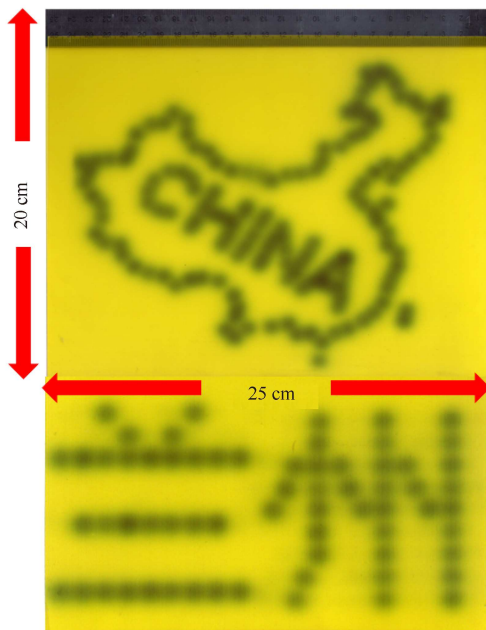
Fig. 6. Arbitrary contours such as a Chinese map and the Chinese characters of Lanzhou shaped by the spot-scanning technique.

The capability of creating uniform irradiation fields by the spot-scanning system for physical and radiobiological experiments was also verified by laterally superposing single Gaussian-shaped beams. The measured data acquired from the horizontal direction of the Φ60 mm field are displayed in Fig. 7 together with the calculated profile based on the beam spot with initial angular and radial spreads. Clearly, the calculated field profile was in good agreement with the measured data, and a uniform irradiation field suitable for cell exposure was generated by the spot scanning system definitely.
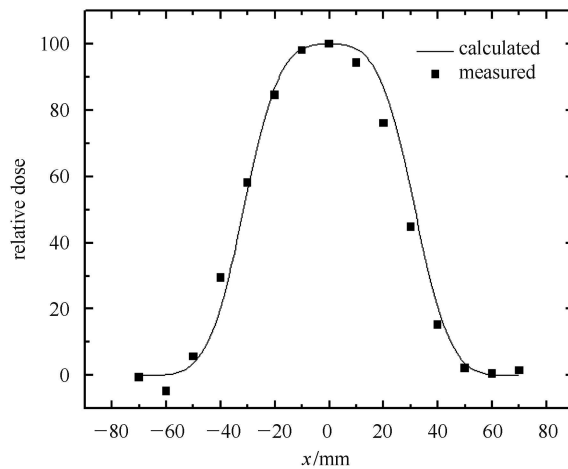
Fig. 7. The lateral profile of the irradiation field in the x direction (squares). The solid line represents the calculated beam profile based on the beam spot with initial angular and radial spreads (the initial Gaussian spot with lateral spread).

3.3 The dose-survival curves

Clonogenic survival fractions against absorbed doses of carbon ions with 50 keV/μm delivered with the spot-scanning and passive methods are displayed in Fig. 8. The measured survival fractions under the two beam delivery methods agreed well with each other except at 2 Gy. But this divergence between the measured data at 2 Gy did not change the tendency that the two dose-survival curves obtained under the two beam delivery methods were analogous. Moreover, no significant difference of the survival fractions was found between the two groups ($p > 0.05$). Because of the similar dose-survival effects obtained under the conditions of active spot-scanning and passive beam deliveries, the equivalence of the newly-developed spot-scanning technique to our previous passive method in terms of biological response at HIRFL-CSR has been proven.
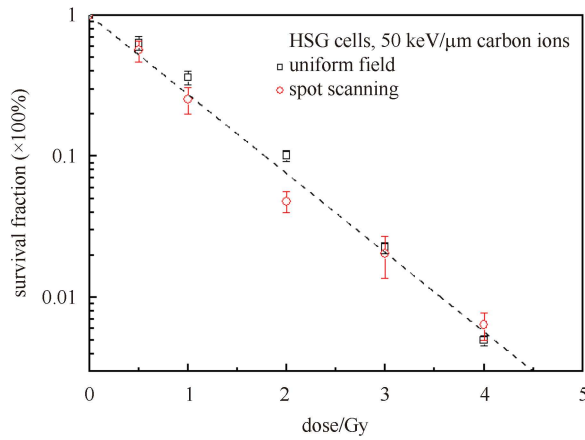
Fig. 8. Clonogenic survival fractions of HSG cells exposed to the carbon ion beams of 50 keV/μm under the passive and spot-scanning beam deliveries.

4   Discussion

Compared with the passive beam-scattering method, active spot-scanning beam delivery is a combination of active energy variation, active beam lateral deflection and beam intensity modulation, which is a rapidly developing technique in particle therapy all over the world [14]. Whether the method of active energy variation is used or not when particle beams are scanned, there is a consensus to choose synchrotron solutions for particle therapy centers presently in operation or under construction such as the projects at PSI, NIRS, GSI and IMP [14–17]. One of the most attractive advantages of the spot-scanning technique is that material in the beam path is minimized as much as possible without energy degraders (absorber plates) and compensators, thus reducing the beam loss and production of secondary particles like neutrons and projectile fragments in front of the patient. Moreover, neither field-specific (all kinds of collimators) nor patient-specific hardware (except for immobilization) is needed while pencil beams sweep as flexibly as an arm directing the fingers. Therefore, any irregular target volumes can be exactly filled with desired doses in principle. This is another one of the most attractive advantages of the spot-scanning technique.

Our active spot-scanning beam delivery system based on the CSR achieved the goal of combining spot-scanning with active energy variation in the tests. The spot-scanning system has preliminarily functioned as expected, because complex contours like the China map and the Chinese characters of Lanzhou were shaped successfully using carbon ions delivered by the system as shown in Fig. 6.

The active energy variation refers to the changeability of beam parameter settings cycle by cycle in accumulation, cooling and acceleration processes of the CSR. An example of the active energy variation cycle by cycle indicated as current signal amplitude is shown in Fig. 9, where the current signals in the successive cycles for carbon ion acceleration were changed so as to lead to energy variation between 150 MeV/u and 300 MeV/u. On the other hand, the ability of the CSR to change beam energy actively was demonstrated through measuring the location shifting of the Bragg peaks of the carbon ion beams with the various energies as shown in Fig. 3.
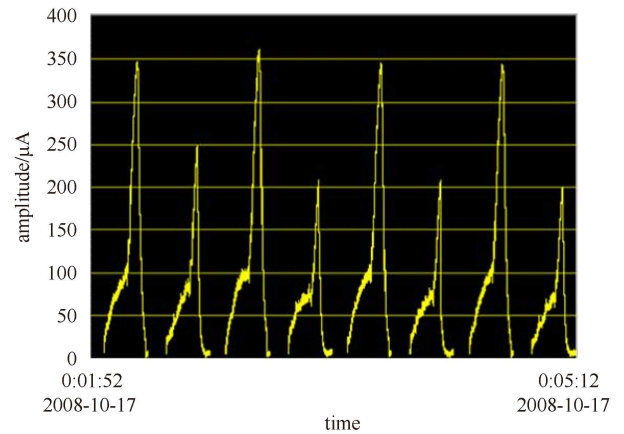
Fig. 9. Active energy variation in successive cycles indicated as current signal amplitude at the CSR synchrotron.

Pencil-like ion beams are driven by scanning magnets, supplied with alterable excitation currents according to the control data, to paint a target volume. So the calibration of steerable beam deflection defined as nominal excitation current is of importance for a spot-scanning system. There are definite linear relationships between the nominal excitation currents for scanning magnets and the lateral deflection position of beam spots at the iso-center for different energy ion beams. The calibration parameters, i.e., slopes and intercepts derived from linear fitting to the measured data for the carbon ion beams at various energies were input into the spot-scanning control system to deflect the carbon ions to the positions expected for them at the iso-center in the tests. To show the functionality of the spot-scanning system to generate irradiation fields, a simple strategy, that is laterally superposing single Gaussian-shaped beam spots with radial spread without particle number optimization for scan points, was applied in this work. As a consequence, a definite two-dimensional dose distribution was achieved as shown in Fig. 7, leading to a uniform

part in the centre of the irradiation field [18]. Compared with the optimization strategy adopted in the treatment planning systems at PSI and GSI [7, 18, 19], this pattern of irradiation field generation by spot scanning is considered to be basic, practical and acceptable for single uniform fields.

The first steps towards an integrated and functional active spot-scanning system have already been taken as shown in the tests herein. Further work on dose optimizations and irradiations to target volumes with the active spot scanning system will be launched in the near future in order to establish a comprehensive technique of active spot-scanning beam delivery in the heavy ion therapy at IMP.

5 Summary

To upgrade and extend the previous passive beam delivery system to an active one, the spot-scanning system as shown in this paper has been developed in the heavy-ion therapy terminal for deep-seated tumor treatment at HIRFL-CSR. Active spot-scanning tests have been carried out as well. The tests show that the condition of performing active spot-scanning beam delivery for heavy ion intensity modulated radiotherapy has already been achieved .

The results and experience obtained in the tests are of great importance for further developing precise spot-scanning techniques for dedicated heavy-ion therapy facilities like the Heavy Ion Tumor Therapy Facility in Lanzhou (HITFiL), which is under construction in Lanzhou.

References

1 Ahlen S P. Reviews of Modern Physics, 1980, **52**: 121
2 Haberer T, Becher W, Schardt D, Kraft G. Nuclear Instruments and Methods in Physics Research Section A: Accelerators, Spectrometers, Detectors and Associated Equipment, 1993, **330**(1–2): 296–305
3 Wilson RR. Radiology, 1946, **47**(5): 487–491
4 Kanai T, Kawachi K, Matsuzawa H, Inada T. Nuclear Instruments and Methods in Physics Research, 1983, **214**(2–3): 491–496
5 Pedroni E, Blattmann H, B hringer T, Coray A, Lin S, Scheib S, Schneider U. Voxel Scanning for Proton Therapy. the NIRS International Workshop on Heavy Charged Particle Therapy and Related Subjects. Proc. of the NIRS International Workshop on Heavy Charged Particle Therapy and Related Subjects. 1991, 94–109
6 Scheib S, Pedroni E. Radiation and Environmental Biophysics, 1992, **31**(3): 251–256
7 Kraft G, Arndt U, Becher W, Schardt D, Stelzer H, Weber U, Archinal T. Nuclear Instruments and Methods in Physics Research Section A: Accelerators, Spectrometers, Detectors and Associated Equipment, 1995, **367**(1–3): 66–70
8 Pedroni E, Bacher R, Blattmann H, B hringer T, Coray A, Lomax A, Lin S, Munkel G, Scheib S, Schneider U. Medical Physics, 1995, **22**: 37

9 Noda K, Furukawa T, Fujisawa T, Iwata Y, Kanai T, Kanazawa M, Kitagawa A, Komori M, Minohara S, Murakami T. Journal of Radiation Research, 2007, **48**(Suppl. A): 43–54
10 LI Q, WEI Z Q, LI W J. Chinese Science Bulletin, 2002, **47**(20): 1708–1710
11 DAI Z Y, LI Q. High Energy Physics and Nuclear Physics, 2007, **31**(7): 655–659 (in Chinese)
12 LI Q, DAI Z Y, YAN Z, JIN X D, LIU X G, XIAO G Q. Medical and Biological Engineering and Computing, 2007, **45**(11): 1037–1043
13 HUANG Y Z, GAO D Q. Atomic Energy Science and Technology, 2009, **9**: 4
14 Schardt D, Elssser T, Schulz-Ertner D. Reviews of Modern Physics, 2010, **82**(1): 383–425
15 Jakel O, Schulz-Ertner D, Karger C P, Nikoghosyan A, Debus J. Technology in Cancer Research and Treatment, 2003, **2**(5): 377–388
16 Sihver L, Mancusi D. Radiation Measurements, 2009, **44**(1): 38–46
17 Urakabe E, Kanai T, Kanazawa M, Kitagawa A, Noda K, Tomitani T, Suda M, Iseki Y, Hanawa K, Sato K. Jpn. J Appl. Phys., 2001, **40**: 2540–2548
18 Kramer M, Jkel O, Haberer T, Kraft G, Schardt D, Weber U. Physics in Medicine and Biology, 2000, **45**: 3299–3317
19 Lomax A. Physics in Medicine and Biology, 1999, **44**: 185